

A PRINTED DISCONE ULTRA-WIDEBAND ANTENNA WITH DUAL-BAND NOTCHED CHARACTERISTICS

X. Li^{*}, H. L. Zheng, T. Quan, and Q. Chen

National Key Laboratory of Antennas and Microwave Technology, Xidian University, Xi'an, Shaanxi 710071, China

Abstract—A printed discone antenna with dual-band notched characteristics is presented for ultra-wideband applications. The proposed antenna consists of a radiation patch which has an outline expressed by binomial function and a trapeziform ground plane. Dual band-stop performance is achieved by etching a pair of Z-shaped slots on the ground plane and protruding a pair of π -shaped strips in the elliptical slot cut in the radiation patch, respectively, which can reject potential interference with the 3.25–3.8 GHz and 5–6 GHz bands. Surface current distributions and input impedance of the antenna are given to analyze the effects of the two resonant structures. The characteristics of the notched bands can be controlled independently by tuning related parameters. Moreover, the performances of the antenna are validated along with simulated and measured results.

1. INTRODUCTION

With the development of modern wireless and mobile communications, the feasible design and implementation of ultra-wideband systems has become a rather competitive topic in both academy and industry communities of telecommunications. As an essential front-end component of the UWB systems, the UWB antenna has received a sparked attention owing to its advantages of broadband impedance matching, stable radiation patterns, and compact size. Nonetheless, the antenna for UWB applications faces the interference with existing narrowband wireless communication systems, such as the IEEE 802.16 WiMAX system operated at 3.3–3.7 GHz and WLAN system operated at 5.15–5.825 GHz. To mitigate the interference with these coexisting systems, it is necessary to endow the UWB antenna with intrinsic filtering properties for rejecting interference.

Received 16 December 2011, Accepted 21 January 2012, Scheduled 26 January 2012

* Corresponding author: Xia Li (girlixia2006@163.com).

In the newly proposed UWB antenna designs, many strategies have been explored to broaden the impedance bandwidth, including properly adding via holes on the microstrip feed-line [1] and extending two symmetrical corrugations from flat ground plane [2]. In [3], a novel monopole antenna with checkered-shaped patch is also proposed for the bandwidth enhancement. To tackle the electromagnetic interference issue mentioned above, one effective approach is to incorporate various resonant structures in the UWB antenna. As a simple type of resonant structure, slot resonator is widely utilized in the designs of band-notched UWB antennas [4, 5]. Parasitic strip is also employed to generate the band-notched feature, which acts as resonator when the length of strip is about a half or a quarter of the guided wavelength at the desired notch frequency [6, 7]. In [8], a novel resonant structure formed by protruding a pair of T-shaped strips inside a square ring radiating patch is proposed.

In this communication, a modified printed discone antenna with dual band-notched characteristics is proposed. As a conventional UWB antenna, the discone antenna possesses the merits of satisfactory impedance bandwidth and omnidirectional radiation patterns. However, it is difficult to miniaturize the antenna structure when integrated with compact RF front ends, which handicaps its further development. To get over this barrier, an effective method is to convert three-dimensional discone antenna into printed monopole antenna [9, 10]. According to this means, the proposed antenna achieves wideband performance of 2.2–16 GHz for VSWR < 2 successfully, covering the entire UWB frequency band (3.1–10.6 GHz). The first notched band, which covers 3.25–3.8 GHz for WiMAX, is achieved by etching a pair of Z-shaped slots on the ground plane. The second notched band, which covers 5–6 GHz for WLAN, is provided by protruding a pair of π -shaped strips inside an ellipse slot cut in the radiation patch. The two notched bands can be effectively tuned by adjusting the dimensions of the slots and π -shaped strips. The design of the proposed antenna is introduced in the second section. The simulated and measured results of the proposed antenna are shown in Section 3. Meanwhile, tuning effects of major geometrical parameters on the performance of the two notched bands are investigated in this section.

2. ANTENNA DESIGN

2.1. UWB Antenna Design

Figure 1 exhibits the schematic diagram of the primitive antenna (referred to as antenna 1), which is mounted on an FR4 substrate

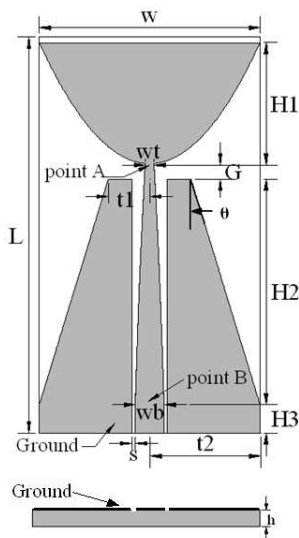


Figure 1. Schematic diagram of the primitive antenna (antenna 1).

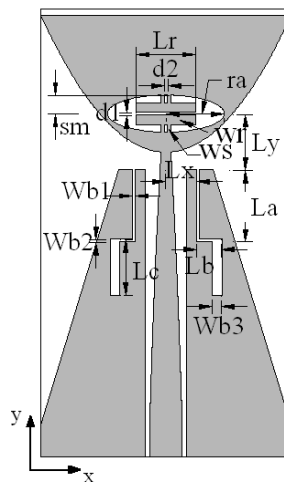


Figure 2. The configuration of the UWB antenna with dual band-notched characteristics (antenna 2).

with thickness of 1.6 mm, relative permittivity of 4.4, a loss tangent of 0.02, and overall size of $36 \times 20 \times 1.6 \text{ mm}^3$. The radiating patch is fed by an exponentially tapered CPW transmission line, in which way the input impedance can be smoothly transformed from 100Ω at point A to 50Ω at point B. The curve of the radiating patch edge is expressed as follows [11]:

$$f(x) = G + H1 \left(\frac{x}{\frac{w}{2}} \right)^2, \quad \frac{wt}{2} \leq x \leq \frac{w}{2} \quad (1)$$

By adjusting the parameters of the length $H1$ and width w of the monopole, the gap width G between the antenna and the ground plane, a favorable impedance matching ($\text{VSWR} \leq 2$) over the entire UWB frequency range (3.1–10.6 GHz) is obtained. Through the combination of rectangular and trapeziform ground plane, and utilizing tapered feed line, the impedance bandwidth of the proposed antenna can be further improved. The electromagnetic simulation software Ansoft HFSS v12 is employed to perform this design. The final optimized parameters are incorporated in Table 1 and the simulated VSWR value of the proposed UWB antenna will be depicted in Section 3.

Table 1. Optimized parameters of antenna 1 and antenna 2 (unit: millimeter).

L	w	$H1$	$H2$	$H3$	wt	wb	G	$t1$	$t2$	s	h	ra	sm
36	20	11	20.5	2.6	0.78	2.6	1.4	3.75	10	0.32	1.6	4.66	1.49
Lr	wr	ws	$d1$	$d2$	Lx	Ly	La	Lb	Lc	$Wb1$	$Wb2$	$Wb3$	
4.8	0.76	0.25	0.13	0.14	0.85	4.5	5.8	1	4.5	0.2	0.2	0.8	

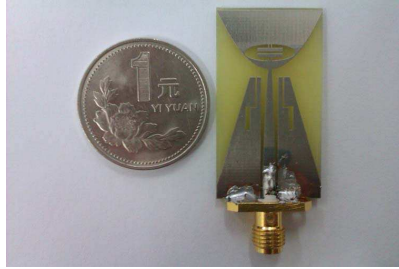


Figure 3. Photograph of the proposed antenna 2.

2.2. Dual Band-notched UWB Antenna Design

To implement dual band-notched function, a pair of Z-shaped slots is etched on the trapeziform ground plane of antenna 1 to yield the first notched band (3.25–3.8 GHz) for WiMAX and a pair of π -shaped strips is protruded in the elliptical slot cut in the radiation patch to generate the second notched band (5–6 GHz) for WLAN. Note that when the band-notched structures applied to antenna 1, there is no need to retune the previously determined parameters. Figure 2 presents the configuration of the proposed UWB antenna with dual band-rejected characteristics (denoted as antenna 2) and its photograph is shown in Figure 3.

The pair of Z-shaped slots symmetrically inserted on the upside of the ground plane is designed according to the following approach. The slot act as a resonator when the length of the slot is about $\lambda_g/4$ (λ_g is the guided wavelength at the desired frequency f_0), which will create destructive interference to the surface current on the ground plane. The guided wavelength can be calculated by

$$\lambda_g = \frac{c}{f_0 \cdot \sqrt{\varepsilon_e}} \quad (2)$$

where c is the speed of the light and ε_e is the effective dielectric constant

which can be calculated by

$$\varepsilon_e = \frac{\varepsilon_r + 1}{2} \quad (3)$$

Taking (2) and (3) into account, the total length of the slot can be obtained approximately in the initial stage.

To realize the second notched band, a pair of π -shaped stubs is protruded inside an elliptical slot etched on the radiator to form a resonator. At resonant frequency, this resonant structure will cause singular input impedance, which causing the desired impedance mismatching near the notch frequency [12]. The mechanism of this resonator will be elaborated in Section 3 by analyzing the surface current distributions near the feed point. The desired notched performance can be obtained by tuning the dimensions of the elliptical slot and the π -shaped stubs.

All the optimized parameters of antenna 1 and antenna 2 are shown in Table 1.

3. RESULTS AND ANALYSIS

3.1. UWB Monopole Antenna

As shown in Figure 4, the printed monopole antenna achieves satisfactory voltage standing wave ratio (VSWR) characteristic within the entire UWB band (3.1–10.6 GHz). There are several factors affecting the impedance bandwidth characteristic, such as feed-gap distance (G) and the inclination-angle (θ) of the trapeziform ground plane. For brevity, main attention is only paid to the effect of varying inclination-angle on the impedance bandwidth. The inclination-angle θ shown in Figure 1 can be calculated by

$$\theta = \text{arctg} \left(\frac{t2 - t1}{H2} \right) \quad (4)$$

Figure 4 reveals the simulated VSWR values for different θ while the other parameters are fixed. It can be drawn that the inclination-angle is a critical parameter to control the low frequency bandwidth. Results show that the low frequency bandwidth can be broaden when θ increases from 6.95 deg to 16.9 deg. This phenomenon can be explained by the characteristic impedance of the discone antenna, which can be obtained by [9]

$$Z_0 \approx 60 \ln \text{ctg} \frac{\theta}{2} \quad (5)$$

In the proposed printed discone antenna, inclination-angle (θ) still plays an important role in the impedance matching. The optimized value of parameter θ is 16.9 deg.

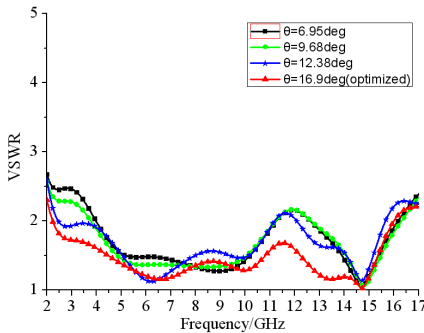


Figure 4. Simulated VSWR values for different θ .

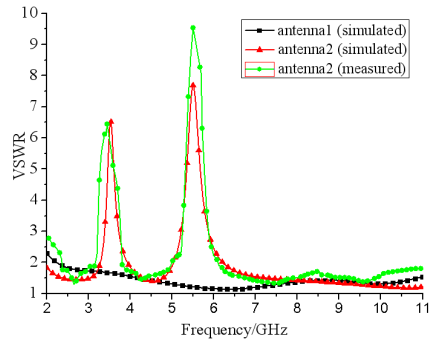


Figure 5. Simulated and measured VSWR of the proposed antenna.

3.2. Primitive Antenna with Desired Band-notched Characteristics

A fabricated prototype for the proposed antenna with band-notched function is constructed and the measured and simulated VSWR versus frequency is illustrated in Figure 5. For comparison, the VSWR of the antenna 1 is also depicted in this figure. It can be observed that the proposed antenna is complying with the desired dual notched bands of 3.25–3.8 GHz and 5–6 GHz, while maintaining excellent impedance matching at other frequencies of UWB band. Therefore, the proposed antenna can suppress any interference with WiMAX system operating at the band of 3.3–3.7 GHz and WLAN system operating at the band of 5.15–5.825 GHz. Compared with the antenna reported in [10], the proposed antenna achieves much sharper band-notched characteristics at the corresponding frequency. As shown in Figure 5, there is tiny discrepancy between simulated and measured results, which is owing to the effects of the SMA port and soldering.

To investigate the band-notched mechanism of the Z-shaped slots and π -shaped stubs structure, the surface current distributions and the input impedance obtained from Ansoft HFSS are given in Figures 6 and 7, respectively.

As shown in Figure 6(a), at the notch frequency 3.5 GHz, the strong resonant current is excited near the perimeters of the slots and is oppositely directed between the interior and exterior of the slots. In this case, relative large energies are captured and stored around the slots, which leads to a large real part of the input impedance as depicted in Figure 6 and a poor impedance matching within the notched band.

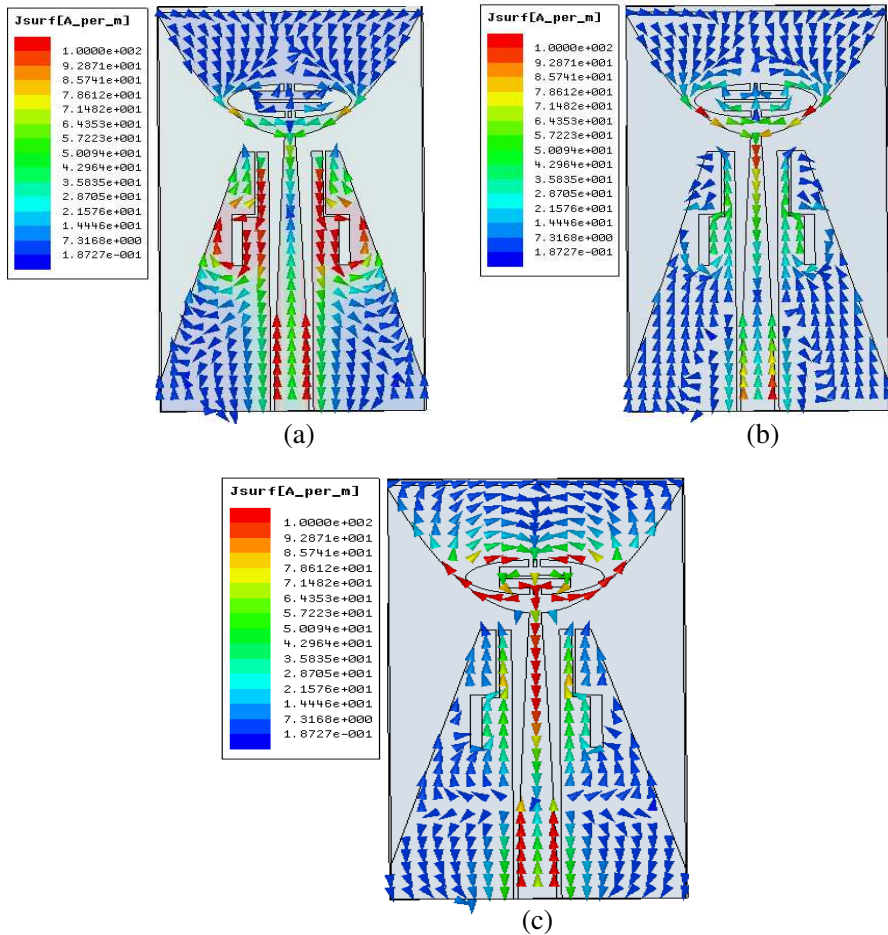


Figure 6. Simulated surface current distributions for antenna 2 at (a) 3.5 GHz, (b) 4.5 GHz, (c) 5.5 GHz.

The resonant structure shown in Figure 2 is formed by protruding a pair of π -shaped stubs inside an elliptical slot cut in the radiator. This resonator can be modeled by a capacitor in parallels with an inductor, in which case the elliptical slot and the π -shaped stubs are equivalent to the inductor and the capacitor, respectively. At the notch frequency 5.5 GHz, the imaginary and real parts of the input impedance are nearly zeros and the current is concentrated on the edge of the elliptical slot and the π -shaped stubs, which can be observed from Figures 6(c) and 7, respectively. This induces the

desired high attenuation near the notch frequency. Through adjusting the electromagnetically coupling between the stubs and the elliptical slot, which is equivalent to tuning the inductor and capacitor values, the desired band-notched performance can be obtained. The resonant structure is placed near the feed point, in which case the rejection performance can be improved significantly. This is due to the fact that the surface current of the antenna 1 corresponding to 5.5 GHz is mainly distributed in the vicinity of the feed point.

Figure 8 depicts the simulated band-rejected feature with varying L_c and $Wb1$. As shown in Figure 8(a), tuning the length of the slots

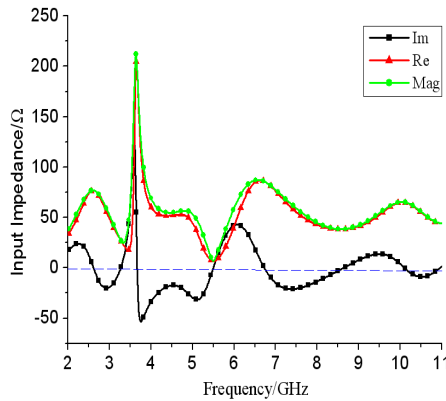


Figure 7. Input impedance of antenna 2.

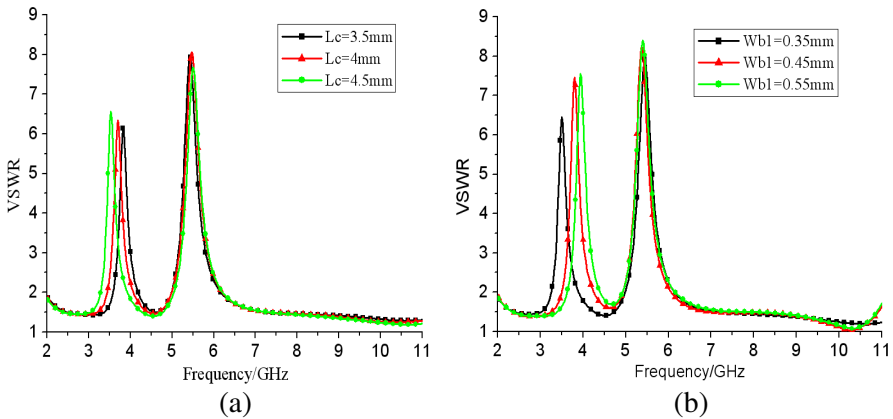


Figure 8. Simulated VSWR for antenna 2 with (a) varying L_c and (b) varying $Wb1$.

can achieve a controllable center-rejected frequency range from 3.5 to 3.85 GHz for the first notched band. Figure 8(b) demonstrates that $Wb1$ is a key factor to control the rejected bandwidth. As the width of the slots increase from 0.35 to 0.55 mm, the bandwidth of the notched band is varied from 0.6 to 0.8 GHz. In Figure 9, the band-notched

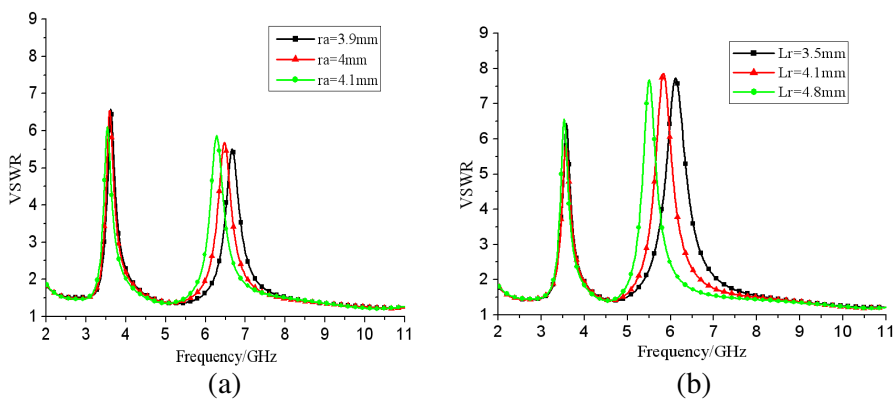
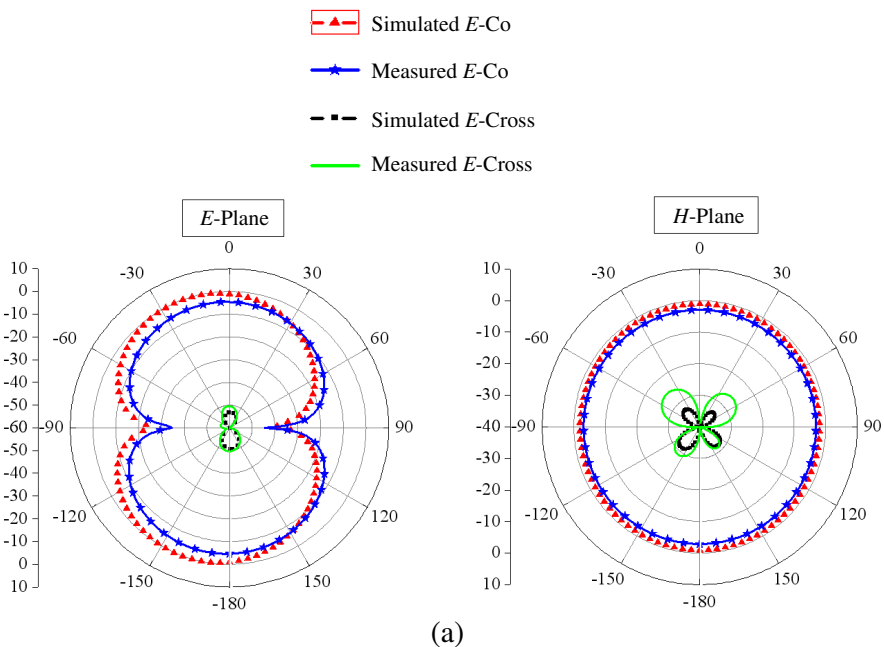


Figure 9. Simulated VSWR for antenna 2 with (a) different ra and (b) different Lr .



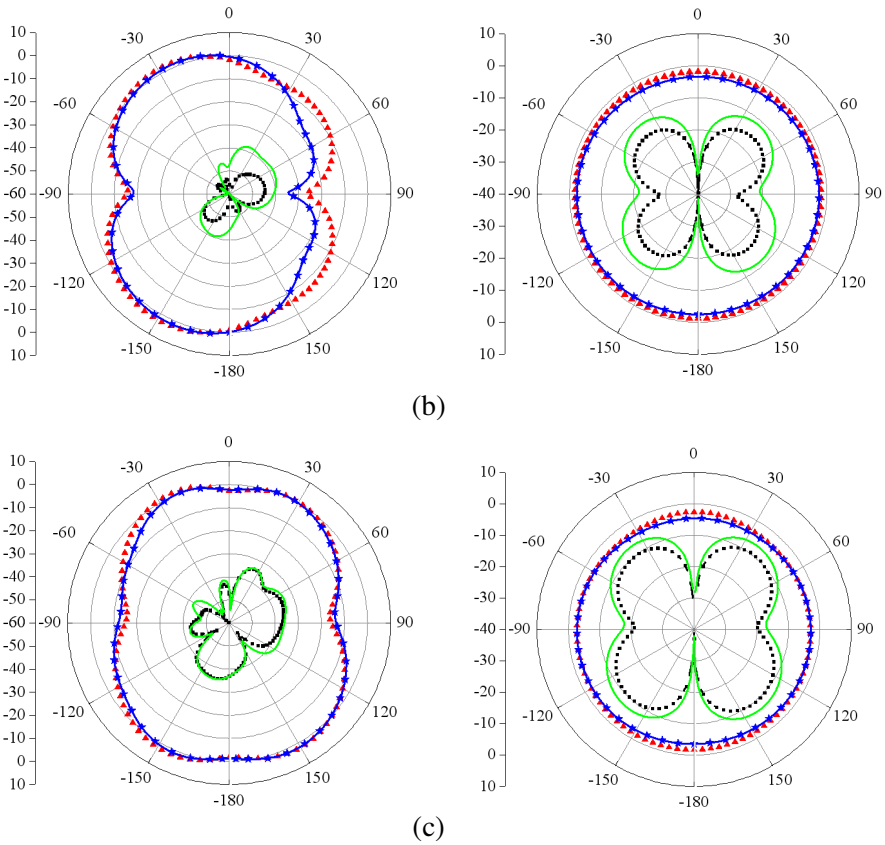


Figure 10. Simulated and measured radiation patterns of antenna 2 at (a) 4 GHz, (b) 7 GHz, (c) 10 GHz.

performance of the second stopband against various ra and Lr is illustrated. It can be seen that an increase in main axis of the elliptical slot with axial ratio fixed at 0.32 results in shifting downwards of the center frequency, which is similar to increasing the inductor value of the parallel LC circuit. On the other hand, the notch bandwidth can be changed by adjusting the length (Lr) of the π -shaped strips. As shown in Figure 9(b), decreasing the value of Lr from 4.8 to 3.5 mm, the notched bandwidth will accordingly increase, which is caused by the increasing of the capacitor value. Consequently, the performance of the dual notched band is tunable and can be controlled independently.

Figure 10 presents the simulated and measured radiation patterns of the proposed antenna with notched bands at frequencies of 4, 7

and 10 GHz in E -plane (yz -plane) and H -plane (xz -plane). It is distinctly revealed from the figure that H -plane patterns are purely omni-directional at all frequencies, while the E -plane patterns similarly exhibit the expected monopole-like behaviors. It's worth noting that applying the Z -shaped slots and the parallel LC resonant circuit to the primitive antenna has little impact on the radiation patterns of the printed monopole antenna. In the notched bands, most of the power fed into the antenna is reflected back, which result in a sharp decrease of the radiation efficiency and the antenna gain. Figure 11 reveals the antenna gain, from which we can see two sharp drops of the antenna gain occur in the frequencies corresponding to the notched bands. For other frequencies outside the notched band, the antenna gain is about the same for the antenna with and without band-notch. As compared to the antenna proposed in [10], it is found that the proposed antenna yields much sharper decrease of the peak gain in the first notched band and higher peak gain in the other frequencies beyond the rejected band. For the same reason illustrated above, the radiation efficiency of the antenna exhibits similar variation can be seen in Figure 12. The characteristics illustrated above indicate that the proposed antenna 2 possesses the ability to suppress interference effectively.

To get an insight into the time domain characteristic of the proposed antenna, the group delay of the proposed antenna is measured between a pair of the proposed antenna in the face-to-face orientation, with a distance of 30 cm between them. For UWB applications, in order to lead little distortions on the signals, the group delay should be constant over the entire operating band. The low-variation of

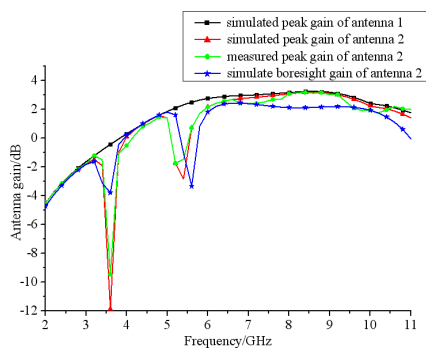


Figure 11. Antenna gain of the proposed antenna.

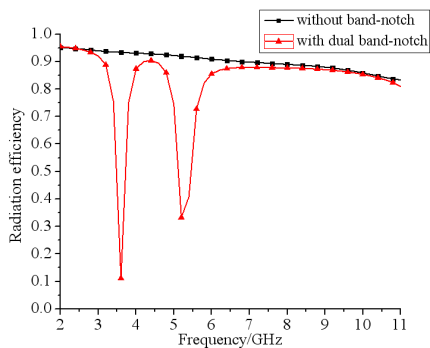


Figure 12. Simulated radiation efficiency of the proposed antenna.

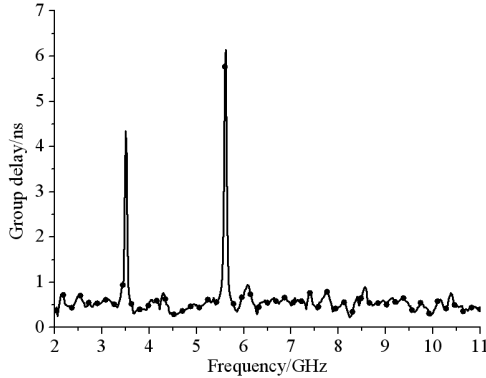


Figure 13. Measured group delay of the proposed antenna.

the group delay outside the notched band, which can be seen in Figure 13, indicates that the proposed antenna exhibits phase linearity at the desired UWB frequencies and hence superior pulse-handling capabilities as demanded by modern communication systems.

4. CONCLUSION

A tapered CPW fed printed disccone antenna with dual band operation for WiMAX/WLAN applications has been presented. The desired band-rejected property is achieved by embedding a pair of Z-shaped resonant slots on the ground and protruding a pair of π -shaped strips in the elliptical slot cut in the radiator. Experimental and measured results reveal the dual notched bands can be tuned flexibly and independently, meanwhile, verify the predicted performance, such as stable radiation patterns and broadband impedance matching across the overall operating frequencies. Hence, the proposed antenna is an excellent candidate for the UWB communication applications.

REFERENCES

1. Chen, D. and C.-H. Cheng, "A novel compact ultrawideband (UWB) wide slot antenna with via holes," *Progress In Electromagnetics Research*, Vol. 94, 343–349, 2009.
2. Lin, C.-C. and H.-R. Chuang, "A 3–12 GHz UWB planar triangular monopole antenna with ridged ground-plane," *Progress In Electromagnetics Research*, Vol. 83, 307–321, 2008.

3. Moosazadeh, M., C. Ghobadi, and M. Dousti, "Small monopole antenna with checkered-shaped patch for UWB application," *IEEE Antennas and Wireless Propagation Letters*, Vol. 9, 2010.
4. Sun, J.-Q., X.-M. Zhang, Y.-B. Yang, R. Guan, and L. Jin, "Dual band-notched ultra-wideband planar monopole antenna with M- and W-slots," *Progress In Electromagnetics Research Letters*, Vol. 19, 1–8, 2010.
5. Li, C.-M. and L.-H. Ye, "Improved dual band-notched UWB slot antenna with controllable notched bandwidths," *Progress In Electromagnetics Research*, Vol. 115, 477–493, 2011.
6. Yazdi, M. and N. Komjani, "A compact band-notched UWB planar monopole antenna with parasitic elements," *Progress In Electromagnetics Research Letters*, Vol. 24, 129–138, 2011.
7. Chen, H., Y. Ding, and D. S. Cai, "A CPW-FED UWB antenna with WIMAX/WLAN band-notched characteristics," *Progress In Electromagnetics Research Letters*, Vol. 25, 163–173, 2011.
8. Ojaroudi, M., S. Yazdanifard, N. Ojaroudi, and R. A. Sadeghzadeh, "Band-notched small square-ring antenna with a pair of T-shaped strips protruded inside the square ring for UWB applications," *IEEE Antennas and Wireless Propagation Letters*, Vol. 10, 2011.
9. Liang, X.-L., S.-S. Zhong, and W. Wang, "Elliptical planar monopole antenna with extremely wide bandwidth," *Electronics Letters*, Vol. 42, No. 8, Apr. 13, 2006.
10. Li, L., S. Zhong, and M. Chen, "Compact band-notched ultra-wideband antenna using defected ground structure," *Microwave and Optical Technology Letters*, Vol. 52, 286–289, 2009.
11. Ling, C.-W., W.-H. Lo, R.-H. Yan, and S.-J. Chung, "Planar binomial curved monopole antennas for ultrawideband communication," *IEEE Transactions on Antennas and Propagation*, Vol. 55, No. 9, Sep. 2007.
12. Hong, C.-Y., C.-W. Ling, I.-Y. Tarn, and S.-J. Chung, "Design of a planar ultrawideband antenna with a new band-notch structure," *IEEE Transactions on Antennas and Propagation*, Vol. 55, No. 12, Dec. 2007.